

The nearly continuous improvement of discharge characteristics and edge stability with increasing lithium coatings in NSTX

R. Maingi^a, D.P. Boyle^{b,c}, J.M. Canik^a, S.M. Kaye^b, T.H. Osborne^e, C.H. Skinner^b, M.G. Bell^b, R.E. Bell^b, A. Diallo^b, S.P. Gerhardt^b, T.K. Gray^a, W. Guttenfelder^b, M.A. Jaworski^b, R. Kaita^b, H.W. Kugel^b, B.P. LeBlanc^b, J. Manickam^b, D.K. Mansfield^b, J.E. Menard^b, M. Ono^b, M. Podesta^b, R. Raman^e, Y. Ren^b, A.L. Roquemore^b, S.A. Sabbagh^f, P.B. Snyder^d, V.A. Soukhanovskii^g
Email: maingir@ornl.gov

^aOak Ridge National Laboratory, Oak Ridge TN, 37831 USA

^bPrinceton Plasma Physics Laboratory, PO Box 451, Princeton, NJ, 08543 USA

^cPrinceton University, Princeton, NJ USA

^dGeneral Atomics, San Diego, CA USA

^eUniv. of Washington, Seattle, WA USA

^fColumbia University, New York, NY, USA

^gLawrence Livermore National Laboratory, Livermore, CA, USA

The understanding of regimes with 1) high pressure at the top of the H-mode pedestal, and 2) devoid of large ELMs is important for scenario optimization of ITER and future devices. In this paper we present analysis for a sequence of progressively increasing lithium coatings¹ in NSTX, demonstrating the nearly continuous improvement of the pedestal height and width with increasing pre-discharge lithium evaporation². In addition, we observed a nearly monotonic reduction in recycling, decrease in electron transport, and modification of the edge profiles and stability with increasing lithium³. These correlations ran contrary to initial expectations that the beneficial effects would saturate. The relevant scale length for deuterium retention is the implantation depth, which we estimated at 5-10 nm. On the other hand, the lithium evaporation in this experiment ranged from 30-500 nm thickness in the lower divertor, i.e. much larger than the implantation depth. The importance of oxygen in enhancing the deuterium retention is under investigation⁴.

A Type I ELMy H-mode scenario with boronized walls provided reference discharges⁵. To this scenario, increasing amounts of pre-discharge lithium were evaporated into the lower divertor². The evolution of various discharge parameters is shown in Figure 1 as a function of pre-discharge lithium deposition. Panels (a) and (b) show that the divertor D_α and midplane neutral pressure gradually decreased with increasing lithium coatings. Panel (c) shows that the confinement enhancement factor relative to the ITER97 L-mode scaling increased gradually during the coating scan, while the electron pressure (P_e) profile peaking factor decreased nearly monotonically with increasing lithium in panel (d). In addition, the ELM frequency also decreased during the coating scan, with robustly ELM-free discharges obtained when the evaporation exceeded ~ 300 mg.

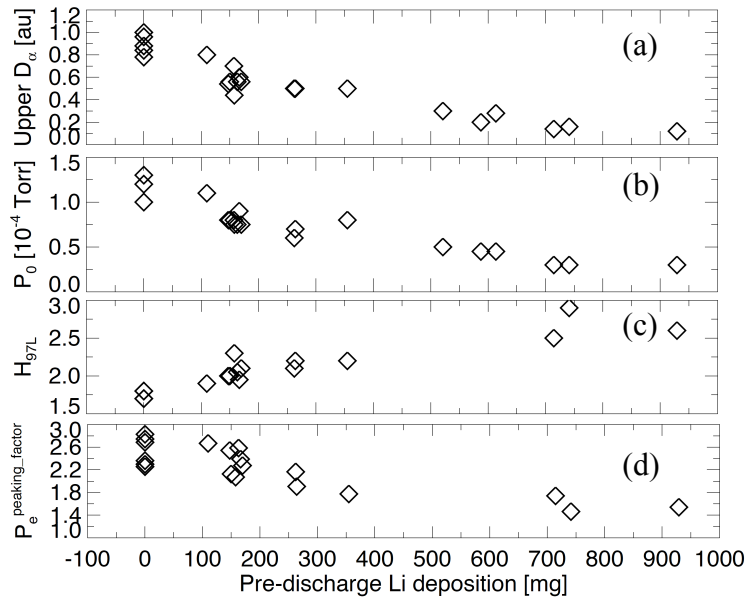


Figure 1: Evolution of discharge quantities as a function of pre-discharge lithium evaporation: (a) divertor D_α , (b) midplane neutral pressure, P_0 , (c) energy confinement relative to ITER97-L scaling at time of peak β_N , and (d) electron pressure profile peaking factor.

Recent interpretive edge transport analysis⁶ with SOLPS and stability analysis³ with ELITE has clarified the mechanism responsible for ELM avoidance: lithium coatings reduce recycling and core fueling; thus the density and its gradient near the separatrix are reduced. The temperature gradient near the separatrix (from $0.95 < \psi_N < 1$) is unaffected; hence the P' and bootstrap current near the separatrix are reduced, leading to stabilization of kink/peeling modes thought to be responsible for the NSTX ELMs. The surprising facet of these data, however, is the growth of the edge transport barrier width, leading to substantially higher plasma pressure at $\psi_N \sim 0.8$, the approximate top of the n_e profile barrier with high pre-discharge evaporation. Figure 2 illustrates the dependence of the n_e , T_e , P_e and total pressure (P_{e+i}) values at two different radial locations, $\psi_N=0.95$ and $\psi_N=0.8$, as a function of pre-discharge lithium. Panel 2a shows that the n_e at $\psi_N=0.95$ decreased with increasing lithium (mostly due to the reduction of the recycling source), but the n_e deeper into the plasma at $\psi_N=0.8$ was relatively unchanged. In contrast, the T_e values at $\psi_N=0.95$ were unchanged, but increased substantially at $\psi_N=0.8$ in panel 2b. The P_e and P_{e+i} values at $\psi_N=0.95$ decreased with the n_e , whereas they increased substantially at $\psi_N=0.8$, following the T_e . Panels 2c and 2d show a P_e (P_{e+i}) threshold of 1 kPa (2 kPa) corresponds to the transition from ELMy to ELM-free operation. Neglecting variations in the separatrix pressure (which is constrained by open field line physics and much smaller than the pedestal pressure in any event), the trend of the pressure at $\psi_N=0.95$ is nearly identical to that of the peak pressure gradient between $0.95 < \psi_N < 1$. Thus, the enhanced edge stability with lithium coatings is correlated with the reduction of the pressure and its gradient from $0.95 < \psi_N < 1$. In qualitative agreement with peeling-ballooning physics, the pedestal width and pedestal top pressures increase substantially with the reduction of P' .

The key ingredient for ELM avoidance is control of the particle channel independent of the thermal channel from $0.95 < \psi_N < 1$. The density profile is continuously manipulated via the amount of lithium evaporation, via recycling control leading to reduced neutral fueling. Transport analysis² (TRANSP), profile analysis^{3, 7} for the fitted pedestal profiles, and edge stability analysis³ (ELITE) of the entire lithium coating variation will be presented. *Research sponsored by the U.S. Dept. of Energy under contracts DE-AC05-00OR22725, DE-AC02-09CH11466, DE-FC02-04ER54698, DE-AC52-07NA27344, DE-FG03-99ER54527 and DE-FG02-99ER54524.

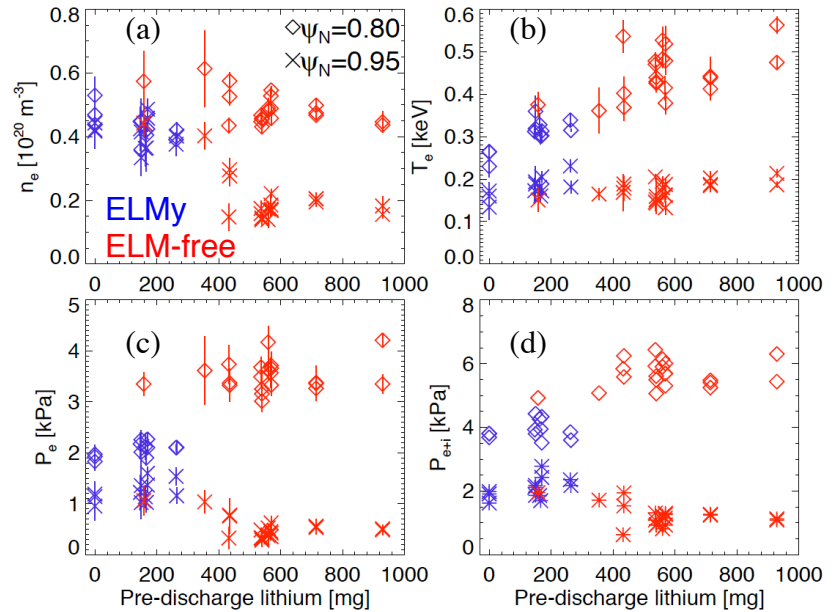


Figure 2: Near-separatrix ($\psi_N=0.95$) and radially inward ($\psi_N=0.8$) values of (a) n_e , (b) T_e , (c) P_e , and (d) P_{e+i} as a function of pre-discharge lithium evaporation. The red and blue data are from time slices without and with ELMs, respectively.

References:

- 1 Kugel H. W., *et al. J. Nucl. Mater.* **415**, S400(2011).
- 2 Maingi R., *et al. Phys. Rev. Lett.* **107**, 145004(2011).
- 3 Boyle D. P., *et al. Plasma Phys. Control. Fusion* **53**, 105011(2011).
- 4 Taylor C. N., *et al. J. Nucl. Mater.* **415**, S777(2011).
- 5 Maingi R., *et al. Nucl. Fusion* **51**, 063036(2011).
- 6 Canik J. M., *et al. Phys. Plasmas* **18**, 056118(2011).
- 7 Maingi R., *et al. Nucl. Fusion* **52**, submitted(2012).